Published in final edited form as:
*Dev Biol*. 2009 January 15; 325(2): 363–373. doi:10.1016/j.ydbio.2008.10.030.

# The cell adhesion molecule Tag1, transmembrane protein Stbm/Vangl2, and Lamininα1 exhibit genetic interactions during migration of facial branchiomotor neurons in zebrafish

**Vinoth Sittaramane**[a,b], **Anagha Sawant**[a], **Marc A. Wolman**[c,d,1], **Lisa Maves**[e], **Mary C. Halloran**[c,d], and **Anand Chandrasekhar**[a,b,f,*]

[a] Division of Biological Sciences and Bond Life Sciences Center, University of Missouri, Columbia, MO 65211, USA

[b] Interdisciplinary Neuroscience Program, University of Missouri, Columbia, MO 65211, USA

[c] Department of Zoology, University of Wisconsin, Madison, WI 53706, USA

[d] Department of Anatomy, University of Wisconsin, Madison, WI 53706, USA

[e] Division of Human Biology, Fred Hutchinson Cancer Research Center, Seattle, WA 98109, USA

[f] Genetics Area Program, University of Missouri, Columbia, MO 65211, USA

## Abstract

Interactions between a neuron and its environment play a major role in neuronal migration. We show here that the cell adhesion molecule Transient Axonal Glycoprotein (Tag1) is necessary for the migration of the facial branchiomotor neurons (FBMNs) in the zebrafish hindbrain. In *tag1* morphant embryos, FBMN migration is specifically blocked, with no effect on organization or patterning of other hindbrain neurons. Furthermore, using suboptimal morpholino doses and genetic mutants, we found that *tag1*, *laminina1* (*lama1*) and *stbm*, which encodes a transmembrane protein Vangl2, exhibit pairwise genetic interactions for FBMN migration. Using time-lapse analyses, we found that FBMNs are affected similarly in all three single morphant embryos, with an inability to extend protrusions in a specific direction, and resulting in the failure of caudal migration. These data suggest that *tag1*, *lama1* and *vangl2* participate in a common mechanism that integrates signaling between the FBMN and its environment to regulate migration.

### Keywords

Hindbrain; Motor neuron; Branchiomotor; Neuronal migration; Time-lapse imaging; Cell adhesion molecule; Tag1; Van gogh-like; Laminin; Genetic interaction

*Corresponding author. Room 340D Bond Life Sciences Center, 1201 E. Rollins Street, University of Missouri, Columbia, MO 65211-7310, USA. Fax: +1 573 884 9676. AnandC@missouri.edu (A. Chandrasekhar).
[1]Current address: Department of Cell and Developmental Biology, University of Pennsylvania, Philadelphia, PA 19104, USA.

**Authors' contributions**

V.S. designed and performed all experiments except those indicated, analyzed the data, and co-wrote the manuscript. A.S. performed the time-lapse experiments and behavioral analysis. L.M. characterized the *bashful*$^{b765}$ allele, and performed the *tri; bal* double mutant experiments. M.A.W. and M.C.H. performed the Tag1 immunostaining experiment, and *tag1* knockdown in the *bashful*$^{uw1}$ background. All authors contributed to the manuscript preparation. A.C. conceived the project, supervised the experiments and co-wrote the manuscript. All authors read and approved the final manuscript.

## Introduction

Migration of newborn neurons from the germinal zone to their final positions is a critical step in the development of a functional nervous system. Defective neuronal migration can lead to severe impairments including mental retardation, epilepsy and learning disabilities (Marin and Rubenstein, 2003). Neuronal migration is largely dependent on the ability of the migrating neurons to interact with adjacent cells to sense and respond to migration cues. Cell migration involves the protrusion of a leading edge process and the formation of adhesion sites at the front while simultaneously contracting and releasing adhesions at the rear (Porcionatto, 2006). Adhesion sites are generated by interactions between cell adhesion molecules (CAMs) and extracellular matrix (ECM) molecules. CAMs play critical roles in various developmental processes, including axon pathfinding and neuronal migration (Sobeih and Corfas, 2002). Transient Axonal Glycoprotein 1 (Tag1), a glycophosphatidylinositol-anchored glycoprotein CAM, is a well-studied member of the immunoglobulin superfamily (Furley et al., 1990) with six immunoglobulin (Ig) domains followed by four fibronectin type III domains (Freigang et al., 2000). The Tag1 CAM plays a significant role in the tangential migration of neurons in the caudal medulla (Denaxa et al., 2005), and the neocortex in mouse (Denaxa et al., 2001). Tag1 also functions in the superficial migratory stream that produces the lateral reticular and external cuneate nuclei in mouse (Kyriakopoulou et al., 2002), and regulates growth cone behaviors of sensory neurons and interneurons in zebrafish (Liu and Halloran, 2005; and Wolman et al., 2008). *tag1* is expressed in the migrating facial branchiomotor neurons (FBMNs) in the mouse and zebrafish hindbrain (Chandrasekhar et al., 1997; Warren et al., 1999; and Garel et al., 2000); however, its role in tangential migration of FBMNs has not been examined.

ECM molecules also regulate neuronal migration. Laminins are a major family of extracellular matrix glycoproteins that typically function as permissive cues for axon outgrowth and neuronal migration (Liesi et al., 1992, 1995; Kuhn et al., 1995, 1998; Adams et al., 2005; and Paulus and Halloran, 2006). Laminins are heterotrimeric protein complexes consisting of α, β and γ subunits, each of which has several isoforms (Colognato and Yurchenco, 2000; Libby et al., 2000; and Miner and Yurchenco, 2004). Laminins are required for cerebellar granule cell migration (Selak et al., 1985; and Liesi et al., 1995). Importantly, laminins can modulate a neuron's response to extracellular guidance molecules (Hopker et al., 1999; and Weinl et al., 2003). In zebrafish, *laminin**α**1* (*lama1*) is required for guidance of retinal ganglion and nucMLF growth cones (Karlstrom et al., 1996; Paulus and Halloran, 2006; and Wolman et al., 2008). In addition, *lama1* plays a role in facial branchiomotor neuron (FBMN) migration (Paulus and Halloran, 2006).

Branchiomotor neurons are generated in specific rhombomeres of the vertebrate hindbrain, and innervate muscles of facial expression, chewing, and vocalization (Lumsden and Keynes, 1989; and Chandrasekhar, 2004). In zebrafish, facial branchiomotor neurons (FBMNs) are born in rhombomere 4 (r4) and migrate caudally (tangentially) into r6 and r7 (Chandrasekhar et al., 1997; Higashijima et al., 2000; and Chandrasekhar, 2004). Several membrane proteins (Stbm/Vangl2, Celsr2, and Fzd3a) have been identified as necessary for FBMN migration (Bingham et al., 2002; and Wada et al., 2006). Interestingly, all of these molecules function non-cell autonomously for FBMN migration (Jessen et al., 2002; and Wada et al., 2006), and little is known about how these molecules function on cells surrounding the FBMNs to regulate their migration. We report here that the cell surface protein Tag1 is necessary for FBMN migration. Furthermore, *tag1*, *stbm*/*vangl2* and *lama1* exhibit strong genetic interactions for FBMN migration, and FBMN migratory behaviors are affected in a similar fashion in *tag1*, *stbm*, *lama1* and morphants. These results indicate that *tag1*, *stbm*, and *lama1* may regulate a common pathway in migrating FBMNs, and offer an approach to elucidate cell autonomous mechanisms underlying FBMN migration.

## Materials and methods

### Animals

Zebrafish (*Danio rerio*) were maintained following standard protocols and university ACUC guidelines as described previously (Westerfield, 1995; and Bingham et al., 2002). For analysis of facial branchiomotor neuron (FBMN) migration, *Tg(isl1:gfp)* fish, which expresses GFP in branchiomotor neurons (Higashijima et al., 2000), were crossed into mutant backgrounds. The following mutant lines were employed in these studies: *trilobite* ($tri^{tc240a}$, Hammerschmidt et al., 1996; and $tri^{m209}$, Solnica-Krezel et al., 1996); and *bashful* ($bal^{b765}$, L.M., unpublished data; and $bal^{uw1}$, Paulus and Halloran, 2006). Embryos were developed at 28.5 °C and staged by hours post fertilization (hpf) (Kimmel et al., 1995).

### Immunohistochemistry and in situ hybridization

Immunohistochemistry was performed according to standard protocols described previously (Chandrasekhar et al., 1997; and Bingham et al., 2002) using the following antibodies: acetylated α-tubulin (Chitnis and Kuwada, 1990; Sigma, 1:500 dilution), zn5 (Trevarrow et al., 1990, Developmental Studies Hybridoma Bank (DSHB),1:10 dilution), tyrosine hydroxylase (Guo et al.,1999; Chemicon/Millipore, 1:500 dilution), GFP (Vanderlaan et al., 2005; Invitrogen, 1:1000 for DAB reaction and 1:4000 for FITC labeling), 3A10 (Hatta, 1992; DSHB, 1:500 dilution), Laminin1 (Paulus and Halloran, 2006; Sigma, 1:400 dilution) and TAG1 (Lang et al., 2001; 1:500 dilution). Fluorescent immunolabeling was performed using RITC-conjugated secondary antibody (for zn5, α-tubulin and TAG1 antibodies; Jackson Immunochemicals, 1:500), and FITC-conjugated secondary antibody (for GFP antibody; Invitrogen, 1:500). Synthesis of digoxygenin labeled probes and whole mount in situ hybridization were carried out using procedures described previously (Chandrasekhar et al., 1997; and Vanderlaan et al., 2005). Stained embryos were deyolked and mounted in glycerol, and imaged using DIC optics on an Olympus BX60 microscope. At least 10 wild-type and 10 mutant embryos were examined for all comparisons. For confocal imaging, embryos were mounted in glycerol and imaged using an Olympus IX70 microscope equipped with a BioRad Radiance 2000 confocal laser system. Images were processed in Adobe Photoshop to adjust brightness and contrast only.

### Morpholino and mRNA injections

Morpholinos targeting *tag1* (MO1; Liu and Halloran, 2005), *stbm*/*vangl2* (Jessen et al., 2002) and *lama1* (MO1; Pollard et al., 2006) were obtained from Gene Tools (Corvallis, OR) or Open Biosystems (Huntsville, AL). For each MO, we performed at least two dose–response experiments to determine the doses that either resulted in a majority of embryos with normal or intermediate FBMN migration phenotypes (suboptimal dose; Figs. 2B, D) or completely blocked FBMN migration (optimal dose; Figs. 2C, D). Intermediate migration phenotypes spanned a spectrum of defects ranging from incomplete (partial) migration out of r4, with FBMNs found throughout the migratory pathway from r4 to r7 on both sides of the hindbrain (Figs. 2B, 5C, E) to relatively normal migration on one side of the hindbrain and an almost complete block of migration on the other side (Fig. 5B). We estimated the dose per embryo based upon the concentration of the MO solution, and the diameter (volume) of the injection bolus in the yolk cell. We typically injected 3–4 nl per embryo. The following doses (suboptimal, optimal) were used: *tag1* MO (6 ng; 12 ng); *stbm* MO (2 ng, 4 ng); and *lama1* MO (1 ng, 2 ng). For the rescue experiments with *tag1* RNA (Fig. 3), a dose of 9 ng *tag1* MO was used. For the genetic interaction experiments (Figs. 5–8), we co-injected two MOs at the sub-optimal doses. For single MO experiments, controls were either uninjected embryos or embryos injected with a standard control MO (7–10 ng) from Gene Tools (5′-CCTCTTACCTCAGTT-ACAATTTATA). Since the control MO did not affect FBMN migration (Fig. 8), many experiments included only uninjected embryos as controls.

For the double MO experiments, controls included injection of single MOs with an appropriate amount of the control MO to match the total MO dose of the double MO-injected embryos. Embryos injected with a suboptimal dose of one MO alone or co-injected with control MO exhibited identical FBMN phenotypes (data not shown), indicating that the enhancement of FBMN migration defects seen in double MO-injected embryos (Fig. 8) is not a non-specific effect of increasing MO dose.

Since we observed increased cell death in *tag1* morphants at the optimal (12 ng) but not suboptimal (6 ng) dose, *p53* MO was co-injected with *tag1* MO in a 1.5:1 ratio to block *p53*-induced apoptosis (Robu et al., 2007). The FBMN migration defect was similar between *p53+tag1* MO-injected and *tag1* MO-injected embryos (data not shown), indicating that the migration defect is not a non-specific effect of the *tag1* MO dose. Data shown in Figs. 2 and 4 are from embryos injected with *tag1* MO alone and *tag1 + p53* MOs, respectively.

Capped *tag1* mRNA was synthesized using the mMessage mMachine Kit (Ambion) from a template lacking the first 20 nucleotides of the 25 nt morpholino binding site in the 5′UTR. The mRNA was checked for purity and size by gel electrophoresis and estimated by UV spectrometry, and ~600 pg was injected into 1–2 cell stage embryos as described previously (Vanderlaan et al., 2005).

### In vivo time-lapse analysis of gfp-expressing migrating motor neurons

At 16–17 hpf, *Tg(isl1:gfp)* embryos were mounted dorsally in 1.2% agarose, bathed in E3 medium containing 0.002% tricaine (Sigma) to anesthetize the embryo, and supplemented with 10 mM HEPES to buffer the pH around the embryo during extended time-lapse observations. The embryos were aligned such that the r4–r5 (caudal) direction was always pointing to 3 o'clock. *Gfp*-expressing motor neurons in rhombomere 4 were selected for imaging in all cases, so that the behavior of FBMNs in wild-type embryos could be compared to the behavior of FBMNs that fail to migrate out of r4 in *tag1*, *stbm*, and *lama1* morphant embryos. Images were acquired at two-minute intervals using Cytos (ASI, Eugene, OR) on an Olympus BX60 microscope equipped with shutters in the fluorescence and bright-field paths. Recordings were performed at ~28 °C, the health and FBMN migration phenotype of embryos were checked at 36 hpf, and data from sickly embryos and those with weakly penetrant migration phenotypes (e.g., Fig. 2B) were excluded from the analysis. FBMN behaviors were analyzed and motility parameters were computed using DIAS software (Solltech, Iowa City, IA). The speed, length-width ratio (LWR), and rate of area change (RAC) for each cell were computed for every two-minute interval, and the mean values over the entire observation period (typically 40–60 min) were pooled for 15 cells within every treatment condition. RAC is defined as the total area of protrusion and retraction of a cell divided by the time interval between frames (2 min), and is a measure of dynamic changes in cell area (i.e., cell activity). Caudal directionality is the ratio of the distance traveled by the cell in the caudal direction to the total distance traveled. Caudal speed is the product of caudal directionality and cell speed, and is a measure of the cell's movement toward r5. Rate of direction change was determined manually by calculating the number of 90° changes in centroid direction (Fig. 9) per 10 min during the observation period.

## Results

### tag1 is expressed in the facial branchiomotor neurons (FBMNs)

*tag1* encodes a GPI-anchored cell adhesion molecule that is expressed transiently in a variety of neurons, and may regulate cell–cell or cell–matrix interactions affecting intracellular signaling (Brummendorf and Rathjen,1996; and Warren et al.,1999).

Expression of *tag1* in facial branchiomotor neurons (FBMNs) was previously reported in zebrafish and mouse (Warren et al., 1999; and Garel et al., 2000). We examined *tag1* expression in detail in the zebrafish hindbrain, and found that putative FBMNs expressing *tag1* were located in rhombomeres 5 and 6 (r5–r6) at 18–19 hpf (Fig. 1A). At 24 hpf, most of the expressing cells were found in r5–r6 (Fig. 1C), coinciding with the period of extensive FBMN migration (Fig. 1B). Interestingly, labeling with anti-Tag1 antibody (Lang et al., 2001) showed that while FBMN axons expressed Tag1 along their entire length inside the hindbrain, only a few FBMN cell bodies in r6 and r7 expressed Tag1 (Fig. 1D), suggesting that protein expression on cell bodies may be limited to the earliest motor neurons to migrate out of r4.

## tag1 is necessary for the tangential migration of FBMNs in zebrafish

Since *tag1* is expressed in migrating FBMNs, we tested whether *tag1* is essential for this process by knocking down its expression using antisense oligonucleotide morpholinos (MO) (Liu and Halloran, 2005; and Wolman et al., 2008). *Tg(isl1:gfp)* embryos were used for these experiments, and FBMN cell bodies and axons were stained using anti-GFP antibody. Injection of *tag1* MO caused a dose dependent loss of FBMN migration (Fig. 2D). At a moderate dose (6–9 ng), FBMN migration was impaired but not blocked (Fig. 2B), whereas at a high MO dose (12 ng), FBMNs mostly failed to migrate (Fig. 2C). Many motor neurons appear to be located in r5 (see also Fig. 4B). However, this displacement does not result from tangential migration since caudally migrating FBMNs form a characteristically curved axon fascicle, the facial genu (Fig. 2A; arrow), which is missing in *tag1* morphants (Fig. 2C).

To test whether the *tag1* morphant phenotype results from the specific loss of *tag1* expression, we attempted to rescue the FBMN phenotype by expressing full-length *tag1* mRNA in MO-injected embryos. Again, *Tg(isl1:gfp)* embryos were used, and FBMN cell bodies and axons were stained using anti-GFP antibody. Expression of synthetic *tag1* mRNA lacking the MO-binding site did not have any effect on FBMN migration (Figs. 3C, E). Co-injection of *tag1* mRNA and *tag1* MO (9 ng) led to a significant reduction in the number of embryos with blocked FBMN migration (Figs. 3B, D, E), demonstrating the specificity of the *tag1* morphant phenotype.

## Neuronal development in tag1 morphants

There was appreciably more cell death in *tag1* morphant hindbrains compared to wild-type embryos (Figs. 4C, D), even after co-injection of *p53* MO to reduce non-specific effects (Robu et al., 2007; see Materials and methods), indicating that the *tag1* MO dose used (12 ng) may be slightly toxic. Nevertheless, hindbrain patterning and development were largely unaffected in morphant embryos. Hindbrain commissural neurons and their axons, labeled with the zn5 antibody (Trevarrow et al., 1990), are located at rhombomere boundaries and mostly developed normally in *tag1* morphants (42/58 embryos) in a similar fashion to wild-type embryos (61/61 embryos) (Figs. 4A, B). *Krox20* (Oxtoby and Jowett, 1993) expression in r3 and r5 was similar in wild-type ($n$=30) and morphant embryos ($n$=26) (Figs. 4I, J). The ventrocaudal migration of noradrenergic locus coeruleus neurons from the cerebellum into r1, assayed by anti-tyrosine hydroxylase (TH) antibody (Guo et al., 1999), occurred normally in *tag1* morphants ($n$=60), as in wild-type embryos ($n$=54) (Figs. 4K, L). Mauthner cells, which are located in r4 and extend decussating axons into the spinal cord, also developed normally in *tag1* morphants (data not shown). These data suggest strongly that the *tag1* morphant hindbrain develops normally, with specific effects on FBMN migration.

Since *tag1* is expressed in cells such as the nucMLF neurons, the trigeminal sensory neurons, and the lateral line ganglion neurons, in addition to the FBMNs (Warren et al.,

1999), we examined their development in *tag1* morphants by tubulin immunostaining. The dorsal and medial longitudinal fascicles (DLF and MLF; Chitnis and Kuwada, 1990) developed normally in *tag1* morphants (Figs. 4E, F, H). Lateral line ganglion neurons and axons were also unaffected in *tag1* morphants. In contrast, nucMLF neurons exhibited pronounced axon guidance defects following *tag1* knockdown (Figs. 4G, H) as described previously (Wolman et al., 2008). The trigeminal sensory ganglion was also frequently affected in *tag1* morphants. The wild-type ganglion is compact, with tightly clustered cell bodies and peripheral axons extending into the ophthalmic and mandibular regions (Fig. 4G; 35/35 embryos). By contrast, trigeminal cell bodies were widely scattered in *tag1* morphants, with axons extending more broadly over the head (Fig. 4H; 31/35 embryos). These data suggest that *tag1* knockdown leads to guidance and adhesion defects that are limited to a subset of *tag1*-expressing neurons. Together with the effects on FBMN migration in *tag1* morphants, our data suggest strongly that *tag1* functions cell autonomously during neural development.

## tag1, stbm (vangl2) and lamininα1 genetically interact with each other to mediate FBMN migration

Migrating neurons likely regulate their behavior by interacting with cues found on neighboring cells and the extracellular matrix (ECM). The gene encoding the transmembrane protein Stbm/Vangl2 is expressed ubiquitously during the period of FBMN migration (Fig. 1E), and *stbm* (*vangl2*) is required for and functions non-cell autonomously during FBMN migration (Bingham et al., 2002; and Jessen et al., 2002). A broadly expressed ECM molecule, Laminin α1 (Lama1; Fig. 1F), also plays a role in FBMN migration (Paulus and Halloran, 2006). Therefore, we tested whether *stbm* and *lama1* exhibited genetic interactions with *tag1* for FBMN migration.

Two genes can be considered to interact genetically if simultaneous partial knockdown of the two genes generates a synergistic and highly penetrant loss of function phenotype than seen with partial knockdown of either gene alone. We performed extensive dose–response analysis to identify the optimum and suboptimal doses for *tag1*, *stbm*, and *lama1* MOs that would cause complete and partial loss of FBMN migration, respectively (see Materials and methods). The optimum doses were: *tag1* MO (12 ng, Fig. 2D); *stbm* MO (4 ng, data not shown); and *lama1* MO (2 ng, data not shown), and the suboptimal doses were: *tag1* MO (6 ng, Figs. 2B, 5B and 7C); *stbm* MO (2 ng, Figs. 5C and 6C) and *lama1* MO (1 ng, Figs. 6B and 7B). Nearly all uninjected wild-type and control MO-injected (7 ng and 11 ng) embryos exhibited normal FBMN migration (Figs. 5A, 6A, 7A and 8). Co-injection of suboptimal doses of *tag1* and *stbm* MOs has a synergistic effect, leading to complete loss of FBMN migration in a majority of embryos (Figs. 5D and 8). To test further, we injected a suboptimal dose of *tag1* MO into *Tg(isl1:gfp)* embryos from crosses between wild-type and *trilobite*$^{tc24oa}$ (*stbm*$^{-}$; Jessen et al., 2002) homozygous mutant fish (generating 100% heterozygous embryos). While 85% (29/34) of uninjected *tri*+/−(*stbm*+/−) embryos exhibited intermediate migration defects (Figs. 5E and 8), 96% (50/52) of *tag1* MO-injected heterozygotes showed complete loss of FBMN migration (Figs. 5F and 8). These data suggest strongly that *tag1* and *stbm* function together to mediate FBMN migration.

In control experiments, we co-injected suboptimal doses of *stbm* or *tag1* MO with control MO to match the MO dose of *stbm*+*tag1* MO injections (see Materials and methods). In these experiments, the control MO did not exacerbate the intermediate FBMN phenotype generated by injection of suboptimal doses of *stbm* or *tag1* MO alone (data not shown), indicating that the synergistic effect of *stbm*+*tag1* MO co-injection is not an artifact of the amount of MO injected.

Co-injection of suboptimal doses of *stbm* and *lama1* MOs also resulted in complete loss of FBMN migration (Figs. 6D and 8). Next, injection of suboptimal dose of *lama1* MO into *tri* +/−embryos, which show intermediate FBMN phenotype (Fig. 6E), also led to elimination of FBMN migration (Figs. 6F and 8; 28/28 embryos). Finally, we examined *Tg(isl1:gfp)* embryos from a *bal*$^{b765}$ (*lama1*)+/−; *tri* (*stbm*) +/−incross. The embryos were sorted on the basis of trunk (*tri* phenotype) and hindbrain (*bal* phenotype) morphology. The *bal* mutant embryos displayed nearly complete loss of FBMN migration (Fig. 6G; *n*=3) as described previously (Paulus and Halloran, 2006). Importantly, putative double heterozygous embryos were morphologically wild-type, but exhibited complete loss of FBMN migration (Fig. 6H; *n*=7). These results suggest strongly that *stbm* and *lama1* genetically interact during FBMN migration.

Co-injection of suboptimal doses of *lama1* and *tag1* MOs also resulted in complete loss of FBMN migration (Figs. 7D and 8). Next, we injected a suboptimal dose of *tag1* MO into embryos from a *bal* $^{uw1}$+/−incross, and assayed FBMN migration at 30 hpf using *tag1* in situs. While FBMN migration was largely blocked in uninjected *bal* mutants as expected (Fig. 7E; *n*=8), migration was also reduced or eliminated in *tag1* MO-injected putative *bal* heterozygotes (Fig. 7F; *n*=24), suggesting strongly that *tag1* and *lama1* interact genetically during FBMN migration.

### tag1, stbm, and lama1 regulate persistent movement of FBMNs

The genetic interaction data suggest that *tag1*, *stbm*, and *lama1* participate in the same pathway to regulate FBMN migration. Therefore, we examined whether knockdown of function of these genes affected dynamic cellular behavior in similar fashion. GFP-expressing FBMNs in control and morphant embryos (injected with optimum dose) were imaged at 2 min intervals beginning at 18–19 hpf. Behavioral analysis was limited to recordings of cells from embryos that displayed a completely penetrant migration defect at 36 hpf. Since FBMNs fail to move out of r4 in morphant embryos, for control embryos we restricted our analyses to motor neurons located in r4. Several motility parameters were calculated from the processed time-lapse movies (Table 1; see Materials and methods; Supplementary data, Movies 1–8). FBMNs from control and morphant embryos had similar length-to-width ratios, moved at comparable speeds within r4, and displayed similar amounts of protrusive activity (rate of area change). However, as expected, FBMNs in morphant embryos moved very slowly along the rostrocaudal axis toward r5 (caudal speed) compared to control FBMNs due to their inability to maintain a persistent direction (caudal directionality), although *tag1* morphant FBMNs appeared to be less affected (Table 1). This defect resulted from the inability of morphant FBMNs to generate protrusions in a directed (polarized) fashion compared to control embryos (rate of direction change; Fig. 9). Difference images show that whereas control cells preferentially formed protrusions in the caudal direction, with few direction changes (Fig. 9A), morphant embryos generated protrusions in random directions leading to significant direction changes and little net progress toward r5 (Figs. 9B–D). We also examined FBMN behaviors in *tri*+/−embryos injected with suboptimal doses of *tag1* or *lama1* MOs, and observed similar qualitative behavioral deficits (data not shown). These data demonstrate that knockdown of *tag1*, *stbm*, and *lama1* have similar effects on the dynamic behaviors of FBMNs, suggesting that the three molecules may regulate the same cellular process involved in the generation of persistent protrusive activity.

## Discussion

Transiently expressed Axonal Glycoprotein 1 (Tag1) is a well-studied member of the immunoglobulin (Ig) superfamily, and is involved in a variety of developmental processes such as cell adhesion, neurite outgrowth, axon pathfinding and neuronal migration. The role

of Tag1 in each of these processes is complex and can vary in different cellular contexts. Tag1 can mediate cell–cell contacts through homophilic binding on apposed membranes (trans interaction) (Rader et al., 1993; and Felsenfeld et al., 1994) and also by heterophilic interactions with other cell adhesion molecules like L1/NgCAM (Kuhn et al., 1991), NrCAM (Suter et al., 1995), NCAM (Milev et al., 1996), proteoglycans like neurcan and phosphacan and extracellular matrix molecules like tenascinC (Milev et al., 1996). In addition, *tag1* is expressed in the migrating cells of superficial migratory stream of the caudal medulla, and is required for their migration (Kyriakopoulou et al., 2002; and Denaxa et al., 2005). Interestingly, while Tag1 is a GPI-anchored membrane protein, it may be able to regulate intracellular signaling indirectly through its extracellular interactions with transmembrane proteins like L1/NgCAM (Lemmon et al., 1992; Zisch et al., 1995; Brummendorf and Rathjen, 1996; and Law et al., 2008).

We show here that zebrafish *tag1* (Warren et al., 1999) is necessary for FBMN migration. In 24 hpf embryos, Tag1 protein is detected only on the axons and cell bodies of a subset of FBMNs located in r6 and r7, which are likely to be the earliest motor neurons to have migrated out of r4. While FBMNs located in r4 and r5 express *tag1* mRNA, these neurons do not express Tag1 protein. One explanation is that the anti-TAG1 antibody may not recognize putative Tag1 ectodomains released from the surface of FBMNs in r4 and r5. Alternatively, the data suggest that *tag1* expression is regulated post-transcriptionally, which has not been reported previously. Interestingly, migration of all FBMNs is blocked in *tag1* morphants, suggesting that *tag1* knockdown blocks migration of the earliest-migrating ("pioneer") FBMNs (expressing Tag1 protein), which in turn may regulate the migration of later-migrating ("follower") FBMNs (not expressing Tag1 protein). This putative non-autonomous effect on "follower" FBMNs may 1) be mediated by heterophilic interactions between Tag1 on "pioneer" FBMNs and cell adhesion molecules like NrCAM or L1/NgCAM (Brummendorf and Rathjen, 1996) or Contactin1 (Fujita and Nagata, 2007) on "follower" FBMNs, or 2) be independent of Tag1 function.

We observed significant but incomplete rescue of FBMN migration defects in *tag1* morphants injected with full-length wild-type *tag1* mRNA. Since the FN and Ig domains are both necessary for Tag1 homophilic interactions (Tsiotra et al., 1996; Kunz et al., 2002; and Pavlou et al., 2002), the rescuing abilities of variants lacking these domains will reveal the importance of homophilic interactions in Tag1-mediated FBMN migration. Since GPI-anchored proteins like Tag1 can be released into the extracellular matrix, it would be instructive to test the abilities of secreted and membrane-bound forms of Tag1 to rescue FBMN migration given that these forms of Tag1 exhibit different activities in aggregation assays (Pavlou et al., 2002).

In *tag1* morphants, trigeminal (Tg) sensory neurons fail to cluster and are mostly found as isolated cells, whereas these neurons are tightly clustered in wild-type embryos. These data suggest that Tag1 may help maintain the integrity of the ganglion, which is consistent with its potential to interact homophilically and heterophilically with other cell adhesion molecules (Brummendorf and Rathjen, 1996). Tg afferent axons are defasciculated following ectopic Slit or neurotrophin expression (Yeo et al., 2004; and Ozdinler et al., 2004), and Tg peripheral axons are defasciculated following contactin1 knockdown (Fujita and Nagata, 2007), but our observations are the first report of disruption of Tg cell body clustering. Other cell types expressing *tag1* such as the nucMLF in the midbrain and Rohon–Beard sensory neurons in the spinal cord also exhibit specific defects in axon outgrowth in *tag1* morphants (Liu and Halloran, 2005; and Wolman et al., 2008). We have not yet carefully examined in *tag1* morphants the development of other *tag1*-expressing cell types such as retinal ganglion cells, cerebellar neurons, and trunk neural crest cells (Warren et al., 1999).

We have identified strong pairwise genetic interactions between *tag1*, *stbm*, and *lama1* during FBMN migration. Other studies have documented genetic interactions of *stbm* with *pk1a* (encoding a cytoplasmic Stbm-interacting protein; Carreira-Barbosa et al., 2003), *celsr2* (encoding an atypical Cadherin; Wada et al., 2006), and *hdac1* (encoding histone deacetylase 1; Nambiar et al., 2007) for neuronal migration. One caveat of these studies is that co-injecting suboptimal doses of morpholinos against any two genes may generate non-specific artifacts, with FBMN migration being especially sensitive to these effects. However, we believe this is unlikely for two reasons. First, all of the pairwise interactions have also been observed when MO targeted against one gene was injected into embryos heterozygous for hypomorphic or null mutations in the second gene. Second, co-injection of control mismatch MOs with a suboptimal dose of a gene-targeting MO does not exacerbate FBMN migration defects generated by the gene-specific MO alone.

The connection between the identified genetic interactions and the underlying molecular mechanisms is unclear. The parsimonious explanation is that *stbm*, *tag1*, and *lama1* participate in a common mechanism mediating FBMN migration. Moreover, analysis of single cell behaviors by time-lapse imaging indicates that knocking down the expression of any of the three genes leads to similar deficits in the ability of FBMNs to generate protrusions in a specific direction, suggesting again that these genes regulate a singular mechanism underlying a specific cell behavior. It is unlikely that Stbm interacts directly with either Tag1 or Lama1 since the two predicted extracellular loops of Stbm are only 15–18 amino acids long, with little secondary structure (Dr. Dong Xu, Department of Computer Science, University of Missouri, personal communication). Importantly, Stbm functions non-cell autonomously in neuroepithelial cells in the ventral neural tube, including floor plate cells (V.S. and A.C., manuscript in preparation), whereas Tag1 may function cell autonomously on FBMNs; hence, Stbm and Tag1 likely do not interact either in cis or in trans to regulate FBMN migration. Interestingly, other molecules discussed below may provide a link between these disparate but functionally associated membrane proteins.

The cytoplasmic protein Scrb1, which is the zebrafish ortholog of the *Drosophila* apicobasal polarity protein scribble, binds Stbm, is required for FBMN migration, and functions non-cell autonomously for this process (Wada et al., 2005). In *Drosophila*, scribble interacts genetically with αPS3 integrin, a member of the α-integrin gene family, for cell cycle entry (Brumby et al., 2004), raising the possibility that vertebrate *scrb1* may genetically interact with integrin genes during FBMN migration. Importantly, Tag1 and other Ig superfamily members like L1 physically interact with each other in cis, and L1 physically interacts with β1 Integrins (Brummendorf and Rathjen, 1996; Malhotra et al., 1998; and Thelen et al., 2002). Furthermore, Tag1-mediated migratory events in cultured neurons require L1 and β1 Integrin functions (Felsenfeld et al., 1994). These studies suggest that the genetic interactions that we have described between *stbm*, *tag1*, and *lama1* may reflect a fundamental role for β1 Integrins in FBMN migration. Experiments testing this hypothesis are in progress.

## Supplementary Material

Refer to Web version on PubMed Central for supplementary material.

## Acknowledgments

We thank members of our labs for excellent fish care. Work with *bashful*$^{b765}$ (*lama1*$^{-}$) was performed in the lab of Dr. Charles Kimmel (University of Oregon), and L.M. thanks him and his lab for support. We thank Dr. Claudia Stuermer (University of Konstanz) for providing the TAG-1 antibody. The zn5 and 3A10 antibodies were obtained from the Developmental Studies Hybridoma Bank maintained by the University of Iowa, Department of Biological

Sciences. This work was supported by NINDS NRSA 1F31NS054430-01A1 to M.A.W., NIH grants NS042228 to M.C.H. and NS040449 to A.C., and a grant from the University of Missouri System RB07-03 to A.C.

## References

Adams DN, Kao EY, Hypolite CL, Distefano MD, Hu WS, Letourneau PC. Growth cones turn and migrate up an immobilized gradient of the laminin IKVAV peptide. J Neurobiol 2005;62:134–147. [PubMed: 15452851]

Bingham S, Higashijima S, Okamoto H, Chandrasekhar A. The zebrafish *trilobite* gene is essential for tangential migration of branchiomotor neurons. Dev Biol 2002;242:149–160. [PubMed: 11820812]

Brumby A, Secombe J, Horsfield J, Coombe M, Amin N, Coates D, Saint R, Richardson H. A genetic screen for dominant modifiers of a cyclin E hypomorphic mutation identifies novel regulators of S-phase entry in *Drosophila*. Genetics 2004;168:227–251. [PubMed: 15454540]

Brummendorf T, Rathjen FG. Structure/function relationships of axon-associated adhesion receptors of the immunoglobulin superfamily. Curr Opin Neurobiol 1996;6:584–593. [PubMed: 8937821]

Carreira-Barbosa F, Concha ML, Takeuchi M, Ueno N, Wilson SW, Tada M. Prickle 1 regulates cell movements during gastrulation and neuronal migration in zebrafish. Development 2003;130:4037–4046. [PubMed: 12874125]

Chandrasekhar A. Turning heads: development of vertebrate branchiomotor neurons. Dev Dyn 2004;229:143–161. [PubMed: 14699587]

Chandrasekhar A, Moens CB, Warren JT, Kimmel CB, Kuwada JY. Development of branchiomotor neurons in zebrafish. Development 1997;124:2633–2644. [PubMed: 9217005]

Chitnis AB, Kuwada JY. Axonogenesis in the brain of zebrafish embryos. J Neurosci 1990;10:1892–1905. [PubMed: 2355256]

Colognato H, Yurchenco PD. Form and function: the laminin family of heterotrimers. Dev Dyn 2000;218:213–234. [PubMed: 10842354]

Denaxa M, Chan CH, Schachner M, Parnavelas JG, Karagogeos D. The adhesion molecule TAG-1 mediates the migration of cortical interneurons from the ganglionic eminence along the corticofugal fiber system. Development 2001;128:4635–4644. [PubMed: 11714688]

Denaxa M, Kyriakopoulou K, Theodorakis K, Trichas G, Vidaki M, Takeda Y, Watanabe K, Karagogeos D. The adhesion molecule TAG-1 is required for proper migration of the superficial migratory stream in the medulla but not of cortical interneurons. Dev Biol 2005;288:87–99. [PubMed: 16225856]

Felsenfeld DP, Hynes MA, Skoler KM, Furley AJ, Jessell TM. TAG-1 can mediate homophilic binding, but neurite outgrowth on TAG-1 requires an L1-like molecule and beta 1 integrins. Neuron 1994;12:675–690. [PubMed: 7512353]

Freigang J, Proba K, Leder L, Diederichs K, Sonderegger P, Welte W. The crystal structure of the ligand binding module of axonin-1/TAG-1 suggests a zipper mechanism for neural cell adhesion. Cell 2000;101:425–433. [PubMed: 10830169]

Fujita N, Nagata S. Contactin 1 knockdown in the hindbrain induces abnormal development of the trigeminal sensory nerve in *Xenopus* embryos. Dev Genes Evol 2007;217:709–713. [PubMed: 17891416]

Furley AJ, Morton SB, Manalo D, Karagogeos D, Dodd J, Jessell TM. The axonal glycoprotein TAG-1 is an immunoglobulin superfamily member with neurite outgrowth-promoting activity. Cell 1990;61:157–170. [PubMed: 2317872]

Garel S, Garcia-Dominguez M, Charnay P. Control of the migratory pathway of facial branchiomotor neurones. Development 2000;127:5297–5307. [PubMed: 11076752]

Guo S, Brush J, Teraoka H, Goddard A, Wilson SW, Mullins MC, Rosenthal A. Development of noradrenergic neurons in the zebrafish hindbrain requires BMP, FGF8, and the homeodomain protein *soulless*/*Phox2a*. Neuron 1999;24:555–566. [PubMed: 10595509]

Hammerschmidt M, Pelegri F, Mullins MC, Kane DA, Brand M, van Eeden FJ, Furutani-Seiki M, Granato M, Haffter P, Heisenberg CP, Jiang YJ, Kelsh RN, Odenthal J, Warga RM, Nusslein-Volhard C. Mutations affecting morphogenesis during gastrulation and tail formation in the zebrafish, *Danio rerio*. Development 1996;123:143–151. [PubMed: 9007236]

Hatta K. Role of the floor plate in axonal patterning in the zebrafish CNS. Neuron 1992;9:629–642. [PubMed: 1382472]

Higashijima S, Hotta Y, Okamoto H. Visualization of cranial motor neurons in live transgenic zebrafish expressing green fluorescent protein under the control of the islet-1 promoter/enhancer. J Neurosci 2000;20:206–218. [PubMed: 10627598]

Hopker VH, Shewan D, Tessier-Lavigne M, Poo M, Holt C. Growth-cone attraction to netrin-1 is converted to repulsion by laminin-1. Nature 1999;401:69–73. [PubMed: 10485706]

Jessen JR, Topczewski J, Bingham S, Sepich DS, Marlow F, Chandrasekhar A, Solnica-Krezel L. Zebrafish *trilobite* identifies new roles for Strabismus in gastrulation and neuronal movements. Nat Cell Biol 2002;8:610–615. [PubMed: 12105418]

Karlstrom RO, Trowe T, Klostermann S, Baier H, Brand M, Crawford AD, Grunewald B, Haffter P, Hoffmann H, Meyer SU, Muller BK, Richter S, van-Eeden FJ, Nusslein-Volhard C, Bonhoeffer F. Zebrafish mutations affecting retinotectal axon pathfinding. Development 1996;123:427–438. [PubMed: 9007260]

Kimmel CB, Ballard WW, Kimmel SR, Ullmann B, Schilling TF. Stages of embryonic development of the zebrafish. Dev Dyn 1995;203:253–310. [PubMed: 8589427]

Kuhn TB, Stoeckli ET, Condrau MA, Rathjen FG, Sonderegger P. Neurite outgrowth on immobilized axonin-1 is mediated by a heterophilic interaction with L1(G4). J Cell Biol 1991;115:1113–1126. [PubMed: 1720120]

Kuhn TB, Schmidt MF, Kater SB. Laminin and fibronectin guideposts signal sustained but opposite effects to passing growth cones. Neuron 1995;14:275–285. [PubMed: 7531986]

Kuhn TB, Williams CV, Dou P, Kater SB. Laminin directs growth cone navigation via two temporally and functionally distinct calcium signals. J Neurosci 1998;18:184–194. [PubMed: 9412499]

Kunz B, Lierheimer R, Rader C, Spirig M, Ziegler U, Sonderegger P. Axonin-1/TAG-1 mediates cell–cell adhesion by a cis-assisted trans-interaction. J Biol Chem 2002;277:4551–4557. [PubMed: 11733523]

Kyriakopoulou K, de Diego I, Wassef M, Karagogeos D. A combination of chain and neurophilic migration involving the adhesion molecule TAG-1 in the caudal medulla. Development 2002;129:287–296. [PubMed: 11807022]

Lang DM, Warren JT Jr, Klisa C, Stuermer CA. Topographic restriction of TAG-1 expression in the developing retinotectal pathway and target dependent reexpression during axon regeneration. Mol Cell Neurosci 2001;17:398–414. [PubMed: 11178876]

Law CO, Kirby RJ, Aghamohammadzadeh S, Furley AJ. The neural adhesion molecule TAG-1 modulates responses of sensory axons to diffusible guidance signals. Development 2008;135:2361–2371. [PubMed: 18550718]

Lemmon V, Burden SM, Payne HR, Elmslie GJ, Hlavin ML. Neurite growth on different substrates: permissive versus instructive influences and the role of adhesive strength. J Neurosci 1992;12:818–826. [PubMed: 1545241]

Libby RT, Champliaud MF, Claudepierre T, Xu Y, Gibbons EP, Koch M, Burgeson RE, Hunter DD, Brunken WJ. Laminin expression in adult and developing retinae: evidence of two novel CNS laminins. J Neurosci 2000;20:6517–6528. [PubMed: 10964957]

Liesi P, Seppala I, Trenkner E. Neuronal migration in cerebellar microcultures is inhibited by antibodies against a neurite outgrowth domain of laminin. J Neurosci Res 1992;33:170–176. [PubMed: 1453481]

Liesi P, Hager G, Dodt HU, Seppala I, Zieglgansberger W. Domain-specific antibodies against the B2 chain of laminin inhibit neuronal migration in the neonatal rat cerebellum. J Neurosci Res 1995;40:199–206. [PubMed: 7745613]

Liu Y, Halloran MC. Central and peripheral axon branches from one neuron are guided differentially by Semaphorin3D and transient axonal glycoprotein-1. J Neurosci 2005;25:10556–10563. [PubMed: 16280593]

Lumsden A, Keynes R. Segmental patterns of neuronal development in the chick hindbrain. Nature 1989;337:424–428. [PubMed: 2644541]

Malhotra JD, Tsiotra P, Karagogeos D, Hortsch M. Cis-activation of L1-mediated ankyrin recruitment by TAG-1 homophilic cell adhesion. J Biol Chem 1998;273:33354–33359. [PubMed: 9837910]

Marin O, Rubenstein JL. Cell migration in the forebrain. Annu Rev Neurosci 2003;26:441–483. [PubMed: 12626695]

Milev P, Maurel P, Haring M, Margolis RK, Margolis RU. TAG-1/axonin-1 is a high-affinity ligand of neurocan, phosphacan/protein-tyrosine phosphatase-zeta/beta, and N-CAM. J Biol Chem 1996;271:15716–15723. [PubMed: 8663515]

Miner JH, Yurchenco PD. Laminin functions in tissue morphogenesis. Annu Rev Cell Dev Biol 2004;20:255–284. [PubMed: 15473841]

Nambiar RM, Ignatius MS, Henion PD. Zebrafish colgate/hdac1 functions in the non-canonical Wnt pathway during axial extension and in Wnt-independent branchiomotor neuron migration. Mech Dev 2007;124:682–698. [PubMed: 17716875]

Oxtoby E, Jowett T. Cloning of the zebrafish *krox-20* gene (*krx-20*) and its expression during hindbrain development. Nucleic Acids Res 1993;21:1087–1095. [PubMed: 8464695]

Ozdinler PH, Ulupinar E, Erzurumlu RS. Local neurotrophin effects on central trigeminal axon growth patterns. Brain Res Dev Brain Res 2004;151:55–66.

Paulus JD, Halloran MC. Zebrafish bashful/laminin-alpha 1 mutants exhibit multiple axon guidance defects. Dev Dyn 2006;235:213–224. [PubMed: 16261616]

Pavlou O, Theodorakis K, Falk J, Kutsche M, Schachner M, Faivre-Sarrailh C, Karagogeos D. Analysis of interactions of the adhesion molecule TAG-1 and its domains with other immunoglobulin superfamily members. Mol Cell Neurosci 2002;20:367–381. [PubMed: 12139915]

Pollard SM, Parsons MJ, Kamei M, Kettleborough RN, Thomas KA, Pham VN, Bae MK, Scott A, Weinstein BM, Stemple DL. Essential and overlapping roles for laminin alpha chains in notochord and blood vessel formation. Dev Biol 2006;289:64–76. [PubMed: 16321372]

Porcionatto MA. The extracellular matrix provides directional cues for neuronal migration during cerebellar development. Braz J Med Biol Res 2006;39:313–320. [PubMed: 16501810]

Rader C, Stoeckli ET, Ziegler U, Osterwalder T, Kunz B, Sonderegger P. Cell–cell adhesion by homophilic interaction of the neuronal recognition molecule axonin-1. Eur J Biochem 1993;215:133–141. [PubMed: 8344273]

Robu ME, Larson JD, Nasevicius A, Beiraghi S, Brenner C, Farber SA, Ekker SC. p53 activation by knockdown technologies. PLoS Genet 2007;3:787–801.

Selak I, Foidart JM, Moonen G. Laminin promotes cerebellar granule cells migration in vitro and is synthesized bycultured astrocytes. Dev Neurosci 1985;7:278–285. [PubMed: 3836139]

Sobeih MM, Corfas G. Extracellular factors that regulate neuronal migration in the central nervous system. Int J Dev Neurosci 2002;20:349–357. [PubMed: 12175873]

Solnica-Krezel L, Stemple DL, Mountcastle-Shah E, Rangini Z, Neuhauss SC, Malicki J, Schier AF, Stainier DY, Zwartkruis F, Abdelilah S, Driever W. Mutations affecting cell fates and cellular rearrangements during gastrulation in zebrafish. Development 1996;123:67–80. [PubMed: 9007230]

Suter DM, Pollerberg GE, Buchstaller A, Giger RJ, Dreyer WJ, Sonderegger P. Binding between the neural cell adhesion molecules axonin-1 and Nr-CAM/Bravo is involved in neuronglia interaction. J Cell Biol 1995;131:1067–1081. [PubMed: 7490283]

Thelen K, Kedar V, Panicker AK, Schmid RS, Midkiff BR, Maness PF. The neural cell adhesion molecule L1 potentiates integrin-dependent cell migration to extracellular matrix proteins. J Neurosci 2002;22:4918–4931. [PubMed: 12077189]

Trevarrow B, Marks DL, Kimmel CB. Organization of hindbrain segments in the zebrafish embryo. Neuron 1990;4:669–679. [PubMed: 2344406]

Tsiotra PC, Theodorakis K, Papamatheakis J, Karagogeos D. The fibronectin domains of the neural adhesion molecule TAX-1 are necessary and sufficient for homophilic binding. J Biol Chem 1996;271:29216–29222. [PubMed: 8910580]

Vanderlaan G, Tyurina OV, Karlstrom RO, Chandrasekhar A. Gli function is essential for motor neuron induction in zebrafish. Dev Biol 2005;282:550–570. [PubMed: 15890329]

Wada H, Iwasaki M, Sato T, Masai I, Nishiwaki Y, Tanaka H, Sato A, Nojima Y, Okamoto H. Dual roles of zygotic and maternal Scribble1 in neural migration and convergent extension movements in zebrafish embryos. Development 2005;132:2273–2285. [PubMed: 15829519]

Wada H, Tanaka H, Nakayama S, Iwasaki M, Okamoto H. Frizzled3a and Celsr2 function in the neuroepithelium to regulate migration of facial motor neurons in the developing zebrafish hindbrain. Development 2006;133:4749–4759. [PubMed: 17079269]

Warren JT, Chandrasekhar A, Kanki JP, Rangarajan R, Furley AJ, Kuwada JY. Molecular cloning and developmental expression of a zebrafish axonal glycoprotein similar to TAG-1. Mech Dev 1999;80:197–201. [PubMed: 10072788]

Weinl C, Drescher U, Lang S, Bonhoeffer F, Loschinger J. On the turning of *Xenopus* retinal axons induced by ephrin-A5. Development 2003;130:1635–1643. [PubMed: 12620987]

Westerfield, M. The Zebrafish Book. University of Oregon; Eugene, OR: 1995.

Wolman MA, Sittaramane VK, Essner JJ, Yost HJ, Chandrasekhar A, Halloran MC. Transient axonal glycoprotein-1 (TAG-1) and laminin-alpha1 regulate dynamic growth cone behaviors and initial axon direction in vivo. Neural Develop 2008;3:6–16.

Yeo SY, Miyashita T, Fricke C, Little MH, Yamada T, Kuwada JY, Huh TL, Chien CB, Okamoto H. Involvement of Islet-2 in the Slit signaling for axonal branching and defasciculation of the sensory neurons in embryonic zebrafish. Mech Dev 2004;121:315–324. [PubMed: 15110042]

Zisch AHD, Alessandri L, Amrein K, Ranscht B, Winterhalter KH, Vaughan L. The glypiated neuronal cell adhesion molecule contactin/F11 complexes with src-family protein tyrosine kinase Fyn. Mol Cell Neurosci 1995;6:263–279. [PubMed: 7496631]

## Appendix A. Supplementary data

Supplementary data associated with this article can be found, in the online version, at doi: 10.1016/j.ydbio.2008.10.030.

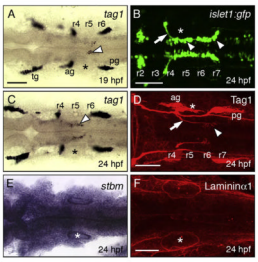


**Fig. 1.**

Expression patterns of *tag1*, *stbm*, and *lama1* in the hindbrain during FBMN migration. All panels show dorsal views of the hindbrain with anterior to the left. Asterisks mark the otic vesicle in each panel. (A, C) *tag1* is expressed in an increasing number of migrating FBMNs (arrowheads) between 19 hpf (A) and 24 hpf (C). Strongest expression is initially found in cells located in r5/r6 (A), and later in cells spanning r5 and r6 (C). (B) In a 24 hpf *Tg(isl1:gfp)* embryo, FBMNs (arrowheads) are found throughout the migratory pathway from r4 to r7, with their axons (arrow) exiting the hindbrain in r4. (D) At 24 hpf, Tag1 immunostaining labels only cell bodies of FBMNs located in r6 and r7 (arrowhead), and their axons (arrow). (E) *stbm* is ubiquitously expressed in the neural tube, and in surrounding non-neural tissues. (F) A 60 μm stack shows broad Laminin1 immunostaining in the basal lamina in the ventral neural tube and adjacent non-neural tissues. tg, trigeminal ganglion; ag, acoustic ganglion; pg, posterior lateral line ganglion. Scale bar in A (75 μm for A, C, E); in B, D, F (75 μm).

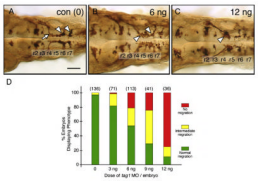


**Fig. 2.**

FBMN migration is affected in *tag1* morphants. Top panels show dorsal views of the hindbrain with anterior to the left. FBMN cell bodies and axons were visualized in *Tg(isl1:gfp)* embryos using anti-GFP antibody. (A) In a 36 hpf control (uninjected) embryo, FBMNs (arrowheads) migrate normally into r6 and r7. (B) An embryo injected with a suboptimal dose (6 ng) of *tag1* MO exhibits an intermediate phenotype, with many FBMNs (arrowheads) remaining in r4 and others migrating into r6 and r7. (C) In an embryo injected with an optimum dose (12 ng), most FBMNs (arrowhead) fail to migrate tangentially out of r4, but many appear to be displaced into r5. (D) Quantification of the *tag1* MO dose–response effect. The green, yellow, and red phenotypic classes correspond to the FBMN migration patterns depicted in panels A–C, respectively. Data from 2–3 experiments; number in parenthesis denotes number of embryos. Scale bar in A (75 μm for A–C).

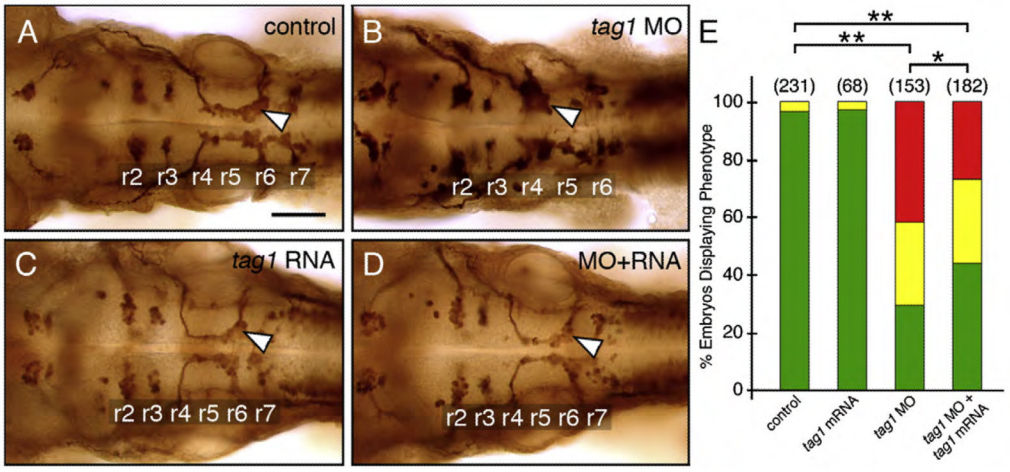


**Fig. 3.**

Rescue of the *tag1* morphant phenotype. Panels A–D show dorsal views of the hindbrain with anterior to the left. FBMN cell bodies and axons were visualized in *Tg(isl1:gfp)* embryos using anti-GFP antibody. Arrowheads indicate FBMNs. (A) FBMNs migrate normally in an uninjected control embryo. (B) FBMNs mostly fail to migrate in a *tag1* morphant embryo. (C) FBMNs migrate normally in a *tag1* mRNA injected embryo. (D) FBMN migration is mostly rescued in an embryo co-injected with *tag1* MO and *tag1* mRNA. (E) Quantification of the rescue data. The distribution of different phenotypes among the various treatments was analyzed by Pearson's Chi-Square statistics. The differences in the phenotypic distributions between the indicated pairs of samples were highly significant (*, $P<0.01$; **, $P<0.001$). Data from 4 experiments. Number in parenthesis denotes number of embryos. Scale bar in A (75 μm for A–D).

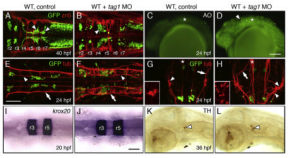

**Fig. 4.**

Neuronal defects in *tag1* morphants. Panels A, B, E–J show dorsal views of the head with anterior to the left (anterior at top in G, H). Panels C, D, K and L show lateral views of the head with anterior to the left. *tag1* morphants (D, F, and H) were co-injected with *p53* MO to minimize non-specific apoptosis (Robu et al., 2007). WT embryos (controls) either uninjected or injected with *p53* MO alone exhibited identical phenotypes in the tissues examined. (A, B) Migration of FBMNs (arrowheads) into r6 and r7 (A) is mostly eliminated in a *tag1* MO-injected embryo (B). Zn5-labeled dorsal commissural neurons (red) at rhombomere boundaries develop in similar numbers in control and morphant embryos. (C, D) While acridine orange (AO) labeling reveals very few dying cells in a control embryo (C), there are many more dying cells (arrowhead) in a *tag1* morphant (D). Asterisk marks otic vesicle. (E) In a control embryo, FBMNs migrate in close proximity to the medial longitudinal fascicle (MLF, arrowhead). Arrow indicates the dorsal longitudinal fascicle (DLF) containing the central (afferent) axons of the trigeminal sensory neurons. (F) In a *tag1* morphant, the MLF (arrowhead) and DLF (arrow) appear brighter, but develop normally. (G, H) The trigeminal sensory ganglion (arrowhead) in a control embryo (G) is compact (inset shows lateral view), with prominent peripheral axons (arrowhead). In contrast, the trigeminal ganglion in a *tag1* morphant (H) is composed of loosely organized cells (arrowheads, and inset showing lateral view), with peripheral axons (arrow) extending broadly over the head. Asterisks indicate the nucleus of the MLF, with brightly-labeled projections in the morphant, compared to the control embryo. (I, J) Expression of *krox20* in r3 and r5 is similar between control and *tag1* morphant embryos. (K, L) Ventrocaudal migration of tyrosine hydroxylase (TH)-positive locus coeruleus neurons (arrowhead) into r1 is similar between control and *tag1* morphant embryos. Scale bar in D (150 μm for C, D); in E (75 μm for A, B, E–H); in J (75 μm for I–L).

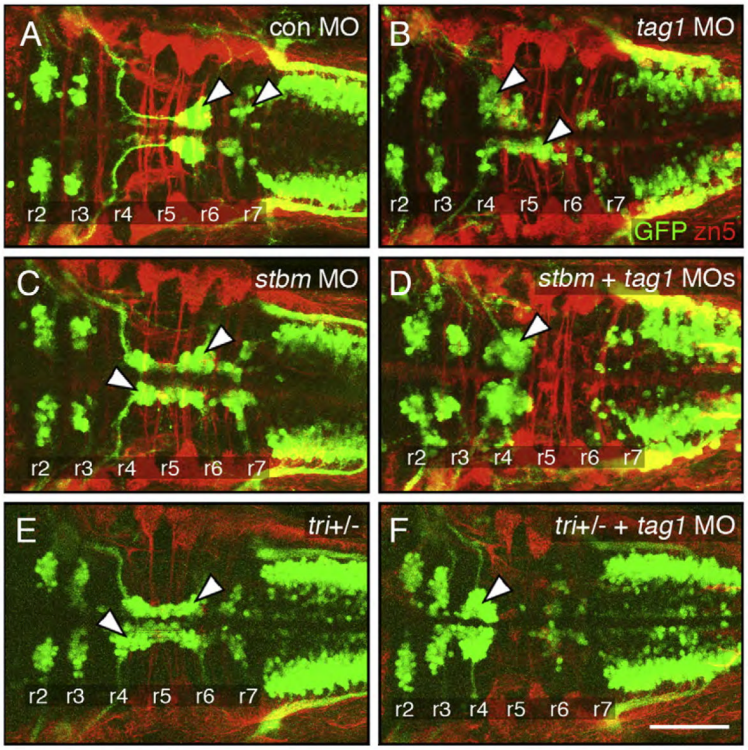


**Fig. 5.**

Genetic interactions between *tag1* and *stbm*. All panels show dorsal views of the hindbrain with anterior to the left. *Tg(isl1:gfp)* embryos were fixed at 48 hpf, and processed for immunohistochemistry with zn5 antibody (red) to label dorsal commissural neurons and axons at rhombomere boundaries, and anti-GFP antibody (green) to label FBMNs (arrowheads). (A) FBMNs migrate normally in a control embryo. (B, C) Partial loss of FBMN migration in embryos injected with suboptimal dose of *tag1* MO (B) or *stbm* MO (C). (D) Complete loss of FBMN migration in an embryo injected with suboptimal doses of *tag1* and *stbm* MOs. (E) Partial loss of FBMN migration in a *trilobite*$^{tc240a}$ (*tri*) heterozygous (*stbm*+/−) embryo. (F) Complete loss of FBMN migration in a *trilobite* heterozygote injected with suboptimal dose of *tag1* MO. Scale bar in F (75 μm for A–F).

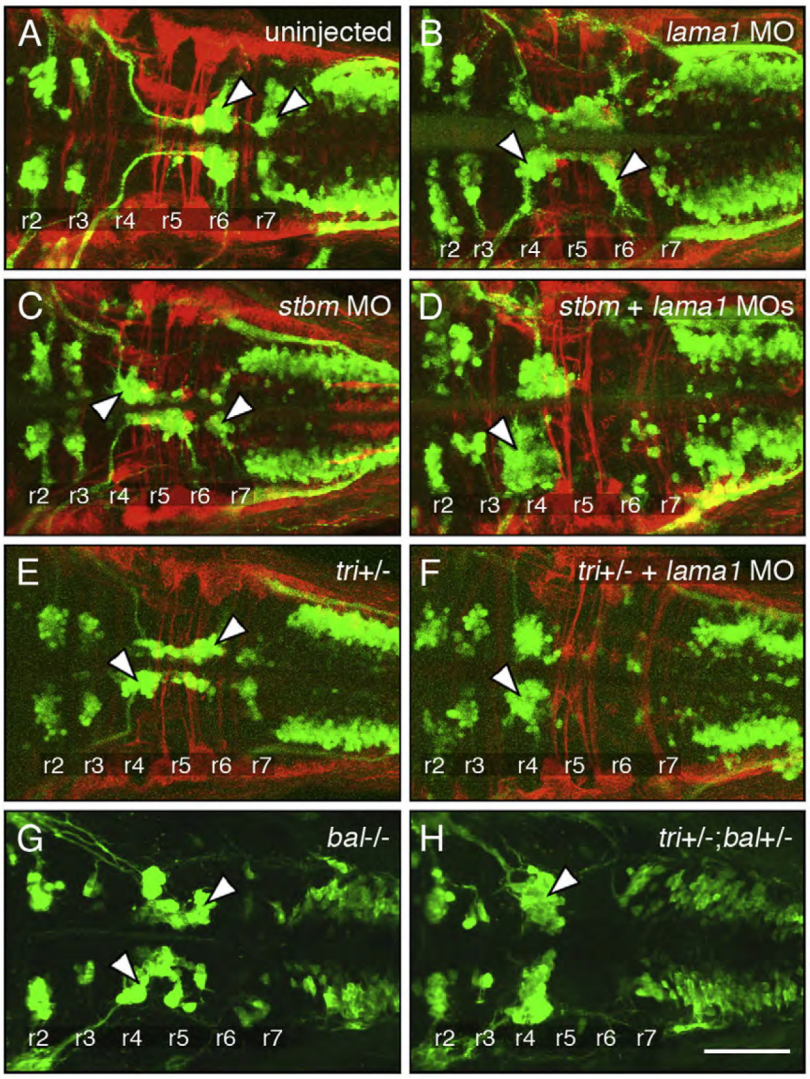


**Fig. 6.**

Genetic interactions between *stbm* and *lama1*. All panels show dorsal views of the hindbrain with anterior to the left. *Tg(isl1:gfp)* embryos were fixed at 48 hpf, and processed for immunohistochemistry with zn5 antibody (red) to label dorsal commissural neurons and axons at rhombomere boundaries (A–F), and anti-GFP antibody (green) to label FBMNs (A–H; arrowheads). (A) FBMNs migrate normally in a control embryo. (B, C) Partial loss of FBMN migration in embryos injected with suboptimal dose of *lama1* MO (B) or *stbm* MO (C). (D) Complete loss of FBMN migration in an embryo injected with suboptimal doses of *lama1* and *stbm* MOs. (E) Partial loss of FBMN migration in a *trilobite*$^{tc240a}$ (*tri*) heterozygous (*stbm*+/−) embryo. (F) Complete loss of FBMN migration in a *trilobite* heterozygote injected with suboptimal dose of *lama1* MO. (G) Greatly reduced FBMN migration in a *bashful*$^{b765}$ homozygous (*lama1*−/−) embryo. (H) Complete loss of FBMN migration in a *trilobite; bashful* double heterozygote. Scale bar in H (75 μm for A–H).

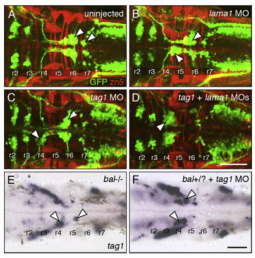


**Fig. 7.**

Genetic interactions between *tag1* and *lama1*. All panels show dorsal views of the hindbrain with anterior to the left. *Tg(isl1:gfp)* embryos (A–D) were fixed at 48 hpf, and processed for immunohistochemistry with zn5 antibody (red) to label dorsal commissural neurons and axons at rhombomere boundaries, and anti-GFP antibody (green) to label FBMNs (arrowheads). Non-transgenic embryos (E, F) were fixed at 30 hpf, and processed for *tag1* in situ hybridization to label FBMNs (arrowheads). (A) FBMNs migrate normally in a control embryo. (B, C) Partial loss of FBMN migration in embryos injected with suboptimal dose of *lama1* MO (B) or *tag1* MO (C). (D) Complete loss of FBMN migration in an embryo injected with suboptimal doses of *tag1* and *lama1* MOs. (E) Greatly reduced FBMN migration in a *bashful*$^{uw1}$ homozygous (*lama1*−/−) embryo. (H) Severe, nearly complete loss of FBMN migration in a putative *bashful* heterozygote injected with suboptimal dose of *tag1* MO. Scale bar in D (75 μm for A–D); in F (75 μm for E, F).

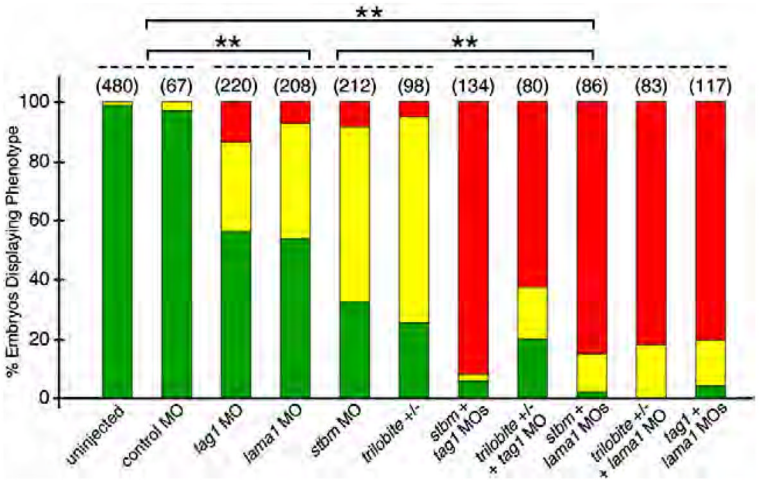


**Fig. 8.**

Quantification of genetic interaction data. Pairwise comparisons were done using Pearson's Chi-square statistics. The differences in the phenotypic distributions between two samples taken from any two of the three different groups (indicated by broken lines) were highly significant (**, $P<0.0001$). Within any group, the differences between any pair of treatments were not significant. Data from 2–6 experiments; number in parenthesis denotes number of embryos.

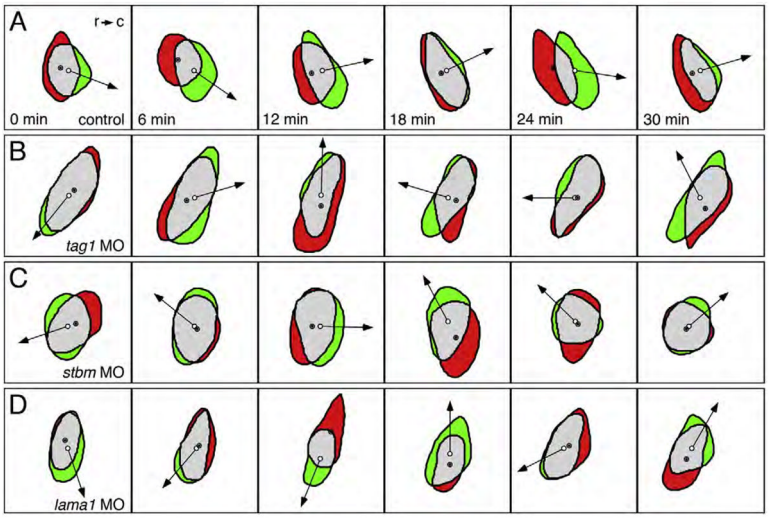


**Fig. 9.**

FBMNs deficient in *tag1*, *stbm* or *lama1* function exhibit non-polarized protrusive activity. Panels show difference images at 6-minute intervals of motor neurons located in r4. Red indicates area of retraction from previous cell position, and green indicates area of protrusion in current cell position. The filled and open circles mark the centroids in the previous and current cell positions, respectively. Arrows point in the direction of cell movement. (A) An FBMN in a control embryo generates protrusions that are biased toward the caudal (c) direction, and retractions that are biased toward the rostral (r) direction, resulting in net caudal translocation of the cell. (B–D) In a *tag1* MO- (B), *stbm* MO- (C), or *lama1* MO- (D) injected embryo, protrusion and retraction areas form in relatively random directions around the periphery of the FBMN. Consequently, the neurons switch directions frequently, resulting in little or no caudal translocation. At least 6 motor neurons were examined by shape analysis for each condition.

## Table 1

Dynamic behaviors of FBMNs located in r4 of wild-type and morphant embryos

| | Control (15 cells) | *tag1* MO (15 cells) | *stbm* MO (15 cells) | *lama1* MO (15 cells) |
|---|---|---|---|---|
| Speed (μm/h) | 19.40±6.72 | 24.05±5.34 | 24.55±8.88 | 22.76±5.46 |
| Length to width ratio (LWR) | 2.03±0.33 | 1.85±0.38 | 2.07±0.67 | 1.97±0.39 |
| Rate of area change ($\mu m^2$/min) | 13.42±1.99 | 12.53±3.67 | 12.18±3.59 | 12.47±2.80 |
| Caudal speed (μm/h) | 8.35±6.48 | 2.70±5.94* | 0.96±5.46* | 0.90±4.80* |
| Caudal directionality | 0.27±0.20 | 0.16±0.32 | 0.01±0.33* | 0.05±0.27* |
| Rate of direction change (# of 90° changes/10 min) | 1.74±0.60 | 2.89±0.56* | 2.77±0.53* | 2.77±0.46* |

See Materials and methods section for definition of parameters and their calculation.

* Highly significant with $p<0.05$ (Student's *t*-test, compared to control). All other parameters were not significantly different between control and experimental embryos.